ORIGINAL ARTICLE

Optimization of pretreatment of potato waste for release of fermentable sugars for vodka production: response surface methodology approach

Deepti Jaswal[1] · Keshani Bhushan[1] · Gurvinder Singh Kocher[1] · Arashdeep Singh[2]

Abstract

Vodka is a transparent distilled alcoholic beverage, obtained by fermenting various substrates such as cereal grains, potatoes, and molasses, offering economic viability and widespread availability. A bioprocess for vodka production was optimized using potato waste collected from Iscon Balaji Foods Pvt. Ltd. Ladhowal, comprising of potato peel, mash, and industrial water. The proximate and physicochemical analysis showed high starch content (59%) and rich organic constituents in potato peel and mash mixture. The response surface methodology was used to optimize liquefaction with α-amylase (5000 IU/mL/min) dose of 0.72% (v/v) for 62.15 min at 59.8 °C and saccharification with glucoamylase (1000 IU/mL/min) dose of 1.7% (v/v) for 28.5 h at 52 °C. The concentration of fermentable sugars in the wort before fermentation was 13.03 mg/mL of total sugars and 10.69 mg/mL of reducing sugars. The ethanol fermentation was carried out by inoculating *Saccharomyces cerevisiae* (MK680910) at the pitching rate of 6% and after 3 days of fermentation the alcohol content of 7.6% (v/v) was recorded in potato waste mixture. Subsequent fractional distillation at 80 °C resulted in ethanol concentration of 38.4% with 76.8° proof. Hence, this study presents an efficient method for fermentative processing of potato waste into vodka.

Keywords Liquefaction · Optimization · Potato waste · Saccharification · Vodka

1 Introduction

Potato (*Solanum tuberosum*) is a globally consumed primary vegetable and a vital food crop, ranking third in production after corn, wheat, and rice [1, 2]. In 2021, worldwide potato production reached 376 million metric tons [3], with India producing 53.58 million metric tons in 2022 [4, 5]. Potatoes are rich in starch and nutrients, including vitamins, minerals, fibre, antioxidants, and phenolic compounds [6, 7]. The food industry utilizes potatoes in various forms such as frozen food, chips, hash browns, and french fries, generating substantial processing waste. Food waste contributes considerably to greenhouse gas emissions, impeding climate change mitigation and jeopardizing food security; around 14% of the world's food is lost or wasted in the supply chain from harvest to sale. As the world's population rises, this poses a significant danger to environmental degradation, food safety, and food security. Fruit and vegetable waste is a major form of food waste, accounting for 0.5 billion tons of the total food waste of 1.3 billion tons annually [8, 9]. Global potato-processing industries generate substantial waste in the form of potato peel, mash/pulp, and wastewater, mainly comprised of starch by-product. Potato peel is the most common by-product of potato processing, consisting of several bioactive compounds, viz., phenolic compounds, glycoalkaloids, polysaccharides, proteins, and vitamins [10] and accounting for 15–40% of the original fresh weight followed by mash and water. Improper waste management increases the risk of microbial contamination, leading to the disposal of significant amounts in landfills, which contributes to

✉ Keshani Bhushan
keshaniplp@gmail.com

✉ Arashdeep Singh
arashrandhawa@pau.edu

Deepti Jaswal
deepti-2151010@pau.edu

Gurvinder Singh Kocher
gskocher@pau.edu

1 Department of Microbiology, Punjab Agricultural University, Ludhiana, Punjab, India 141004

2 Department of Food Science and Technology, Punjab Agricultural University, Ludhiana, Punjab, India 141004

increased greenhouse gas emission [11]. Apart from using potato industry by-products as animal feed [12], it has also been used for the extraction of bio-functional components and production of high-value products such as snacks, waffles, and powders which primarily use potato peel and mash [8, 13].

Waste potato peels and mash having zero market value is generated in large amounts by potato-processing industries. Currently, the waste from the potato industry is primarily utilized as animal feed. However, it can also be used for ethanol and vodka production as it serves as an economical carbon source for fermentation as it contains considerable amount of starch and fermentable sugars [14]. Waste potato mash, comprising 80% moisture, and potato peel, containing 25% starch with low fermentable sugars [2], can be utilized for ethanol fermentation.

However, the brewing yeast utilized in the fermentation process lacks the ability to directly hydrolyze starch. Before the fermentation process takes place, it is necessary to undergo a series of steps in which fermentable sugars are generated from starch through either enzymatic hydrolysis or acid hydrolysis, specifically known as liquefaction and saccharification [15, 16]. Currently two hydrolysis methods, acidic and enzymatic, are used by the industries, with a preference for enzymatic hydrolysis. Acidic hydrolysis presents drawbacks such as the potential inhibition of yeast growth, the need for neutralization, and also the requirement for corrosion-resistant materials [17]. Enzymatic hydrolysis, despite being a more cost-effective option, is preferred due to its superior conversion yield of glucose [18, 19].

Microbial amylases, particularly α-amylase and glucoamylase, play a key role in breaking down starch into fermentable sugars during the hydrolysis process [17]. By optimizing the dosage of these enzymes in liquefaction and saccharification processes, the fermentation industries can reap benefit by utilizing potato waste for ethanol production. Fadel [20] and Liimatainen [21] also demonstrated that potato industry wastes can be a potential carbon source for yeast in alcohol fermentation.

Response surface methodology (RSM) is the most widely used multivariate statistical tool for optimizing food operations [22]. RSM is a combination of statistical and mathematical procedures based on fitting a polynomial model to data in order to make statistical predictions for model development, measuring the influence of numerous independent variables, and obtaining the optimal values of variables [23]. The RSM approach method is beneficial for optimizing, creating, developing, and enhancing food processes such as extraction, drying, blanching, enzymatic hydrolysis and clarifying, manufacturing, and formulation, when a response or reactions are influenced by several factors [24, 25]. Box-Behnken, a subset of RSM, simplifies the process with fewer samples and replicates by examining quadratic effects of factors post-screening factorial experiments. This cost-effective design is widely used in food processing and is appropriate for evaluating factor interactions and studying processes without extreme points. Hence, this study aimed to optimize the liquefaction and saccharification conditions for potato waste (comprising potato mash, peel, and industrial water) using the RSM approach to achieve the highest ethanol yield for vodka production.

2 Materials and methods

2.1 Raw materials

Potato waste, comprising peel, mash, and industrial water, was sourced from Iscon Balaji Foods Pvt. Ltd. in Ladhowal, Ludhiana, Punjab. Peel and mash were dried overnight at 50 ± 2 °C in a tray drier and then milled to 500–1000 µm particle size using a blender (Inalsa Star Juicer Mixer Grinder) which was packed in polypropylene bags and stored at refrigeration temperature until further use [26]. The study optimized the dosage of α-amylase (enzyme concentrations used were 5000 IU/mL/min) for the liquefaction and glucoamylase (enzyme concentrations used were 1000 IU/mL/min) for saccharification of starch. Both enzymes were purchased from Alfanzyme (Belgaum/Karnataka, India).

2.2 Proximate analysis

The moisture, ash, cellulose, hemicellulose, lignin, and crude protein content of the potato waste were evaluated as per the methodology [27], starch [28], total sugars [29], and reducing sugar [30].

2.3 Structural characterization

The Fourier transfer infrared (FTIR) spectra of potato waste, both potato mash and potato peel, functional groups were analysed using an FTIR spectrometer. Agilent Cary Model 630FTIR (Agilent Technologies, Santa Clara, CA, USA) was used to acquire FTIR spectra (five scans) of prepared films on ATR (attenuated total reflected) having 8 cm^{-1} resolution within 4000–500-cm^{-1} region [31, 32].

2.4 Optimization of starch hydrolysis process

Response surface methodology (RSM) was used for optimization of liquefaction and saccharification of potato waste to release fermentable sugars. A three-factor, three-level Box–Behnken design was used to optimize the release of total soluble solids (TSS), total sugars (TS), and reducing sugars (RS) in potato waste for three variables. Actual factor levels corresponding to coded factor levels are detailed

in Table 1, determined based on preliminary studies. The optimal conditions for maximum release of TSS, TS, and RS were determined through statistical analysis using Design expert software (Version 11.0., Stat-Ease Inc., Minneapolis, USA). Coefficients in the second-order polynomial were calculated through multiple regression analysis on the experimentally obtained data Table 1.

The response function (Y) was expressed as a polynomial (1), and factors were analysed for linear, quadratic, and interactive components.

$$Y = b0 + b1x1 + b2x2 + b3x3 + b12x1x2 + b13x1x3 \\ + b23x2x3 + b11x12 + b22x22 + b33x32 + \varepsilon \tag{1}$$

where Y is the response, $b0$ is the intercept, b1, b2, b3 represents linear effects, b12, b13, b23 are interactive effects, b11, b22, b33 are quadratic effects and ε is random error. The significance of the model was assessed by the analysis of variance (ANOVA). Statistical analysis, including ANOVA, Fisher's F-test, and correlation coefficients, evaluated the model's significance and goodness of fit. 3D surface plots visually represented quadratic models for each variable.

2.5 Biological culture

Saccharomyces cerevisiae (MK680910) fermentations were conducted using a yeast culture obtained from the Fermentation Laboratory of the Department of Microbiology at Punjab Agricultural University in Ludhiana, Punjab, India. The yeast was cultivated in a general glucose yeast extract (GYE) broth, with the composition of the broth being glucose 10.0 g/L, peptone 5.0 g/L, and yeast extract 5.0 g/L. A loopful of the slant culture was introduced into the sterilized GYE broth to initiate the culture. The seed inoculum was incubated at 28 °C for 24 h at 120 rpm. Subsequently, a starter culture was prepared in a sucrose solution (4%) using 2% of the seed broth. The inoculated sucrose solution was then shaken at 100 rpm for 24 h at 28 °C.

2.6 Fermentation and distillation

A homogeneous slurry was prepared by blending 20 g of mixture comprising of peel and mash in a 1:1 with 140 mL of industrial water in a 1:7 ratio. Slurry was then used in experiments. Following this, the potato slurry was heated to 100 °C for 60 min and left to stand for 10 min for gelatinization. Optimized doses of two enzymes, namely α-amylase (5000 IU/mL/min) and glucoamylase (1000 IU/mL/min), were used for liquefaction and saccharification to release the fermentable sugars. The fermentation process was carried out in sterilized 250-mL Erlenmeyer flasks with a working volume of 150 mL according to the experimental design. Flasks containing pre-treated potato waste slurry, fermentation media inoculated with 6% (v/v) *Saccharomyces cerevisiae* (MK680910), were incubated at 28 °C for 72 h. Further distillation was carried out by using a glass condenser at a temperature of 80 °C for separation of ethanol from other impurities, ensuring efficiency and enhancing the overall quality of the vodka production.

2.7 Statistical analysis

The data was analysed by ANOVA using SPSS Statistical software (version 1.80, SPPS Inc., Chicago, IL, USA). Post hoc analysis using Tukey's b test was conducted to compare means at a significance level of $P < 0.05$.

3 Results and discussion

3.1 Potato waste proximal analysis

The nutritional and proximate composition of potato waste comprising of potato peel and mash separately as well as in the combination with 1:1 ratio is presented in Table 2. Combination of peel and mash had significantly higher moisture ($P < 0.05$), ash, organic matter, crude protein, cellulose, hemicellulose, and carbohydrate content in comparison to the individual samples of potato peel and mash. Azizi et al. [33] found that potato peel powder had a higher ash content than mash powders, suggesting a greater mineral content, and similar results are obtained in our study with the combination having an overall higher ash content followed by potato peel waste. The nitrogen content in the combination as well as peel waste was found to be significantly similar 3.1% and 3.2% with lowest in the potato mash (1.1%). Liang et al. [34] also reported that nitrogen protein

Table 1 The experimental design for liquefaction and saccharification involved selecting specific levels for the factors

Independent variable	Levels	
	Liquefaction	
	− 1	+ 1
Time (min)	55	65
Temperature (°C)	58	62
α-amylase enzyme (5000IU/mL/min) (%v/v)	0.5	0.78
Independent variable	Levels	
	Saccharification	
	− 1	+ 1
Time (h)	20	28
Temperature (°C)	48	52
Glucoamylase (1000 IU/mL/min) (%v/v)	1.4	1.7

Table 2 Proximate composition of the potato waste

Parameters	Moisture (%)	Ash (%)	Organic matter	Crude protein (%)	Nitrogen (%)	Cellulose (%)	Hemicellulose (%)	Lignin (%)	Carbohydrates (%)
Potato peel	6.3 ± 0.10^b	8.3 ± 0.37^b	12 ± 0.26^c	18 ± 0.20^b	3.1 ± 0.10^a	11.0 ± 0.10^c	18.5 ± 0.30^c	7.3 ± 0.10^a	50.2 ± 0.15^c
Potato mash	5.1 ± 0.10^c	3.3 ± 0.15^c	18.5 ± 0.40^b	11.3 ± 0.15^c	1.1 ± 0.10^b	14.8 ± 0.10^a	28.1 ± 0.15^b	2.5 ± 0.15^c	64.7 ± 0.60^b
Potato peel + mash (1:1)	7.1 ± 0.10^a	9.3 ± 0.10^a	19.6 ± 0.15^a	22.0 ± 0.62^a	3.2 ± 0.10^a	15.1 ± 0.15^b	29.4 ± 0.21^a	7.0 ± 0.15^b	73.5 ± 0.45^a

Results are expressed as mean standard deviation (SD) ($n = 3$). Values in the column with different superscripts are significantly different ($P < 0.05$) as assessed by Tukey's b post hoc test

is higher in potato peel in comparison to potato mash. Phenolic acids are the most abundant phenolic compounds in potatoes and constitute 90% of the phenolic compounds in potato peels [35]. The total phenolic content in raw potato peel is reported as 1.02–2.92 g/100 g by [36]. Phenolics are known to negatively affect yeast metabolism during fermentation and show an inhibitory effect on the fermentation activity of yeasts [37]. Hence, it is essential to extract the phenolics from the potato peel waste prior to fermentation for improved fermentation efficiency, while considering the economical viability of the method. The cumulative findings emphasize the potential of utilizing the entire potato waste comprising of peel and mash, as a nutritionally rich and well-balanced resource for fermentation process, possibly contributing to reduced waste and improved sustainability in food utilization.

3.2 Compound characterization of potato waste

FTIR analysis was conducted to identify the functional groups present in potato peel and mash, as depicted in Fig. 1a and b, respectively. The spectra revealed prominent amide I, amide II, and amide III bands at wavenumbers around 1630, 1542, and 1224 cm^{-1}. In both potato peel and mash, the strongest bond in the 3290-cm^{-1} region indicated the stretching of water bonds, signifying moisture absorption [31, 32]. Protein-related vibrations were identified, with amide I absorption attributed to protein amide C=O stretching vibrations at around 1632 cm^{-1} [31, 38]. Amide II absorption was associated with N–H bending and C–N stretching vibrations around 1542 cm^{-1}. The complex amide III band encompassed N–H in-plane bending and C–N stretching induced by amide linkages [39, 40].

The amide I region, marked by sharp peaks at 1636 cm^{-1}, represented the vital C=O stretching vibration mode crucial for analysing protein secondary structure [41]. N–H deformation occurred within the wavenumber range of 1660–1200 cm^{-1}, indicating gelatin fractions. Absorption bands at 1148 and 864 cm^{-1} were associated with C–H and C=C stretching in aromatic compounds [42, 43]. Additionally, peaks at 960–961 cm^{-1}, 1025–1044 cm^{-1}, and 1089–1095 cm^{-1} indicated P–O group stretching vibrations, with the 1000–1100-cm^{-1} region intensifying phosphate bonds in starch [31]. The origin of amide I absorption was attributed to protein amide C=O stretching vibrations, while amide II absorption was characterized by N–H bending and C–N stretching vibrations. The amide III band, a complex feature, was formed by amide connections inducing both
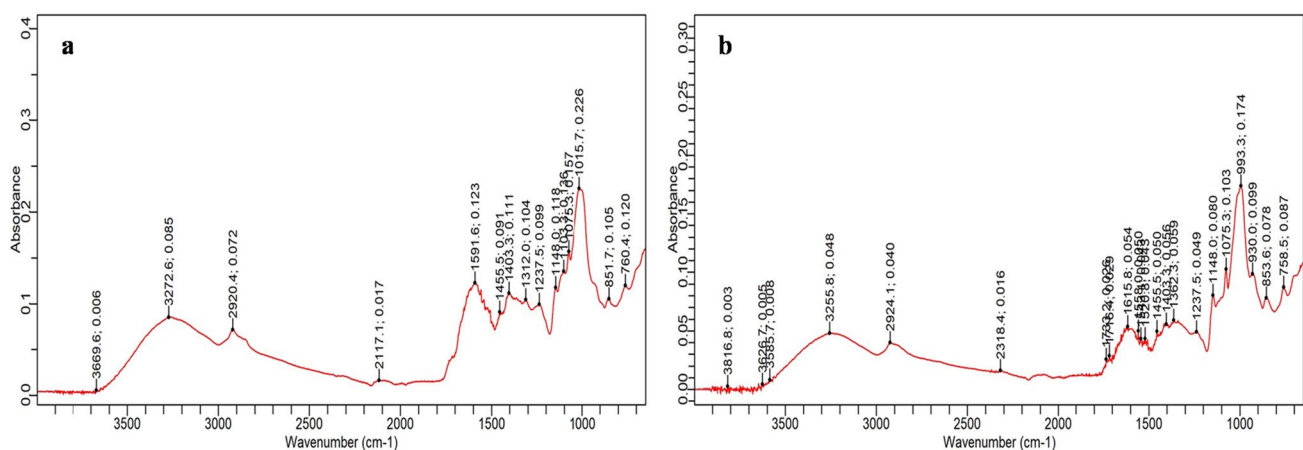
Fig. 1 Fourier transform infrared spectroscopy (FTIR) of potato waste. **a** Potato peel. **b** Potato mash

C–N stretching and N–H plane bending [32]. FTIR analysis provided insights into the molecular composition of potato peel and mash, highlighting the presence of specific functional groups associated with proteins, carbohydrates, and water bonds.

3.3 Development of RSM model

The experimental conditions for liquefaction and saccharification with the corresponding TSS, TS, and RS are presented in Tables 3 and 4. Experimental data were used to formulate three poly nominal equations for liquefaction and saccharification establishing relationships with TSS, TS, and RS with the input variable shown in the equation. Equations are illustrated as (2), (3), (4), (5), (6), and (7).

$$
\begin{aligned}
Y1 = {}& 8.60 + 0.0979A + 0.1178B + 0.5761C \\
& + 0.0750AB + 0.0000AC + 0.1000BC \\
& - 0.5847A^2 - 0.5493B^2 - 0.3195C^2
\end{aligned}
\tag{2}
$$

$$
\begin{aligned}
Y2 = {}& 9.29 + 0.6299A + 0.2597B + 0.6644C \\
& + 0.2410AB + 0.0925AC + 0.1415BC \\
& - 0.4432A^2 - 0.8227B^2 - 0.7614C^2
\end{aligned}
\tag{3}
$$

$$
\begin{aligned}
Y3 = {}& 7.235 + 0.4526A + 0.3356B + 0.48956C \\
& + 0.0105AB + 0.1569AC - 0.0652BC \\
& + 0.1528A^2 - 0.0654B^2 - 0.7089C^2
\end{aligned}
\tag{4}
$$

$$
\begin{aligned}
Y4 = {}& +10.41 + 0.7116A + 0.1395B + 0.5768C \\
& + 0.1750AB + 0.4250AC + 0.1000BC \\
& + 0.1229A^2 - 0.1423B^2 - 0.2483C^2
\end{aligned}
\tag{5}
$$

$$
\begin{aligned}
Y5 = {}& +10.51 + 0.9409A + 0.4387B + 0.6674C \\
& + 0.0115AB + 0.2107AC - 0.0995BC \\
& + 0.2609A^2 - 0.0870B^2 - 0.1098C^2
\end{aligned}
\tag{6}
$$

$$
\begin{aligned}
Y6 = {}& +8.61 + 0.5503A + 0.2473B + 0.3489C \\
& + 0.0718AB + 0.17.03AC + 0.0578BC \\
& + 0.0538A^2 - 0.2031B^2 - 0.1893C^2
\end{aligned}
\tag{7}
$$

where (2)–(7), Y1, Y2, and Y3 denote liquefaction parameters, while Y4, Y5, and Y6 represent saccharification parameters, corresponding to TSS, TS, and RS, respectively. The variables A, B, and C in these equations represent time, temperature, and α-amylase/glucoamylase dose, respectively. The fitted models' validity was assessed through analysis of variance (ANOVA) (Tables 5 and 6). Liquefaction parameters, including TSS, TS, and RS, exhibited high F-values

Table 3 Experimental response profile for optimization of liquefaction

Run	Process variables			Dependent response		
	A, time (min)	B, temperature (°C)	C, α-amylase % (v/v)	TSS (°Brix)	TS (mg/mL)	RS (mg/mL)
1	65	62	0.49	6.9	5.018	4.957
2	65	58	0.49	6.7	4.523	4.327
3	60	63.3	0.68	6.8	4.811	4.524
4	60	60	0.35	6.5	4.193	3.942
5	55	58	0.78	7.4	5.420	5.300
6	60	60	0.64	8.5	7.855	7.012
7	55	58	0.49	6.7	4.242	3.493
8	68.4	60	0.64	7.0	6.047	5.967
9	60	60	0.47	7.6	7.112	6.641
10	55	62	0.64	6.4	4.154	3.638
11	60	59	0.78	8.7	8.409	7.951
12	55	62	0.64	6.4	4.154	3.638
13	60	60	0.64	8.5	7.855	7.012
14	60	56.6	0.64	6.7	4.247	3.493
15	51.5	60	0.64	6.1	4.051	3.112
16	60	60	0.64	8.5	7.855	7.012
17	60	60	0.85	8.6	8.188	7.112
18	65	62	0.78	7.6	6.043	5.576
19	65	58	0.78	7.9	7.601	7.012
20	60	60	0.64	8.5	7.855	7.012

TSS, total soluble solids; *TS*, total sugars; *RS*, reducing sugars

Table 4 Experimental response profile for optimization of saccharification

Run	Process variables			Dependent response		
	A, time (h)	B, temperature (°C)	C, glucoamylase %(v/v)	TSS (°Brix)	TS (mg/mL)	RS (mg/mL)
1	24	50	1.60	10.5	10.958	8.424
2	24	50	1.60	10.0	11.233	8.556
3	24	50	1.60	10.4	10.835	8.363
4	24	50	1.28	8.1	8.767	7.205
5	24	50	1.57	10.5	8.920	8.425
6	24	50	1.85	12.4	11.994	9.119
7	24	50	1.60	10.2	10.893	8.426
8	28	52	1.42	10.1	11.242	8.526
9	20	48	1.78	9.7	9.451	7.564
10	24	50	1.60	10.9	10.654	8.910
11	20	52	1.42	9.8	9.777	7.822
12	24	46.6	1.60	9.7	9.674	7.651
13	20	52	1.78	9.7	10.472	8.212
14	20	48	1.42	9.8	9.145	7.863
15	17.2	50	1.78	8.9	9.357	7.415
16	28	48	1.78	11.0	11.713	8.662
17	28.5	50	1.60	14.8	13.501	10.284
18	24	53.3	1.60	10.0	11.216	8.595
19	28	48	1.42	9.8	9.777	7.822
20	28	52	1.78	12.1	11.993	9.114

TSS, total soluble solids; *TS*, total sugars; *RS*, reducing sugars

Table 5 ANOVA for the response surface of a quadratic model with respect to liquefaction

Source	TSS (°Brix)		TS (mg/mL)		RS (mg/mL)	
	F-value	P-value	F-value	P-value	F-value	P-value
Model	36.66	< 0.0001	91.10	< 0.0001	36.66	< 0.0001
A—time	28.90	0.0003	59.09	< 0.0001	28.90	0.0003
B—temperature	20.24	0.0011	38.23	< 0.0001	20.24	0.0011
C—α-amylase	69.05	< 0.0001	243.50	< 0.0001	69.05	< 0.0001
AB	5.32	0.0437	3.78	0.0805	5.32	0.0437
AC	0.7839	0.3967	0.0151	0.9045	0.7839	0.3967
BC	1.83	0.2054	3.07	0.1101	1.83	0.2054
A^2	32.42	0.0002	112.36	0.0045	32.42	0.0002
B^2	111.72	< 0.0001	330.17	< 0.0001	111.72	< 0.0001
C^2	95.68	< 0.0001	110.63	< 0.0001	95.68	< 0.0001
Lack of fit	1.34	0.4397	5.22	0.6246	2.89	0.1397
Cor total	14.35		60.58		29.69	
Adjusted R^2	0.9681		0.9212		0.9421	
Predicted R^2	0.8875		0.9572		0.9502	
R^2	0.9832		0.9480		0.9706	
Adeq precision	20.5035		82.6733		0.8197	

of 65.10, 91.10, and 36.66, respectively, with corresponding low P-values of < 0.0001, < 0.0001, and < 0.0001. Similarly, saccharification parameters displayed F-values of 6.74, 3.30, and 4.79, with P-values of 0.0031, 0.0384, and 0.0112, respectively. These high F-values and low P-values (< 0.05) underscore the significance of the models. The coefficient of determination (R^2) values for TSS, TS, and RS in both liquefaction and saccharification models were 0.9832, 0.9480,

Table 6 ANOVA for the response surface of a quadratic model with respect to saccharification

Source	TSS (°Brix)		TS (mg/mL)		RS (mg/mL)	
	F-value	P-value	F-value	P-value	F-value	P-value
Model	6.74	0.0031	3.30	0.0384	4.79	0.0112
A—time	28.04	0.0003	15.85	0.0026	22.10	0.0008
B—temperature	1.08	0.3238	3.45	0.0931	4.46	0.0607
C—α-amylase	18.43	0.0016	7.98	0.0180	8.89	0.0138
AB	0.9935	0.3424	0.0014	0.9710	0.2201	0.6490
AC	5.86	0.0360	0.4659	0.5104	1.24	0.2916
BC	0.3244	0.5815	0.1039	0.7539	0.1426	0.7136
A^2	0.8828	0.3696	1.29	0.2831	0.2227	0.6471
B^2	1.18	0.3023	0.1429	0.7133	3.18	0.1050
C^2	3.60	0.0869	0.2277	0.6435	2.76	0.1276
Lack of fit	4.27	0.3397	3.51	0.2246	1.57	0.1654
Cor total	17.42		30.26		9.93	
Adjusted R^2	0.7310		0.9212		0.6421	
Predicted R^2	0.0835		0.9572		0.2502	
R^2	0.9584		0.9726		0.9116	
Adeq precision	10.0605		6.7699		7.4969	

and 0.9706 and 0.9584, 0.9726, and 0.9116, respectively. These R^2 values indicate that the models can explain 92.6% and 98.6% of the observed variation in the data for liquefaction and saccharification, respectively.

The significance of individual parameters was evaluated using P-values from Tables 5 and 6. Time, temperature, and the enzymatic dose of α-amylase exhibited a significant impact on TSS, TS, and RS. Additionally, glucoamylase demonstrated an interactive effect on these parameters. During both liquefaction and saccharification processes, time and temperature primarily influenced enzymatic activity, with lower temperatures hindering enzyme flexibility and higher temperatures causing thermal denaturation [47]. As time decreased, enzymatic activity slowed, impacting enzyme diffusion and potentially reducing sugar release. Optimal times increased enzyme-substrate contact, catalyzing breakdown reactions. However, excessively high enzyme concentrations could lead to overcrowding, thus inhibiting efficiency [44]. Conversely, low enzymatic doses risked incomplete hydrolysis, diminishing process efficiency and fermentable sugar yields.

3.4 Optimization of process parameters for liquefaction by using RSM

3.4.1 Interactive effects of process parameters on TSS, TS, and RS during liquefaction

The TSS, TS, and RS from the various experimental runs are shown in Table 3. TSS varied from 6.2 to 8.7 °Brix, TS from 4.051 to 8.409 mg/mL, and RS from 3.112 to 7.942 mg/mL. At median input values (runs 6, 13, and 20),

all process inputs resulted in consistent outcomes. Alternatively, run 9, conducted under reduced conditions of time (51.5 min), temperature (60 °C), and α-amylase (5000 IU/mL/min) dose (0.64% (v/v)), resulted in significantly lower TSS (6.1 °Brix), TS (4.051 mg/mL), and RS (3.112 mg/mL) respectively. During the extended reaction time of 65 min, elevated temperature at 58 °C, and α-amylase dose of 0.78% (run 19), a significant rise in concentrations was observed, i.e. TSS increased to 7.9 °Brix, TS to 7.601 mg/mL, and RS to 7.012 mg/mL.

The response surface graphs in Fig. 2 illustrate the interactive effects of process parameters on TSS, TS, and RS. A simultaneous increase in time (58 to 60 min) and temperature (58.2 to 60 °C) led to an increase in TSS (7.8 to 8.7 °Brix), TS (7.845 to 8.409 mg/mL), and RS (7021 to 7.951 mg/mL). However, further increases in time (> 65 min) and temperature (> 63 °C) resulted in a decreased TSS, TS, and RS, respectively (Fig. 2A, B, C). Rani et al. [45] optimized liquefaction parameters for potato, obtaining a glucose content of 825.1 mg/g, at 56.4 °C, 1% (v/v) α-amylase concentration, and a 60-min incubation period. Betiku et al. [46] achieved a maximum glucose concentration of 126.66 g/L by optimizing liquefaction conditions using sweet potato peel as a feedstock, including a 60-min liquefaction time, 1% (v/v) α-amylase dosage, and at 56.4 °C. The thermal lysis of α-amylase, occurring at temperatures exceeding 60 °C during the liquefaction process, contributes significantly to the influence of temperature on TSS, TS, and RS. Conversely, operating at lower temperatures, specifically below 55 °C for α-amylase, diminishes enzymatic efficiency, thereby adversely impacting sugar release. To achieve optimal results in the liquefaction processes, it is crucial to adhere
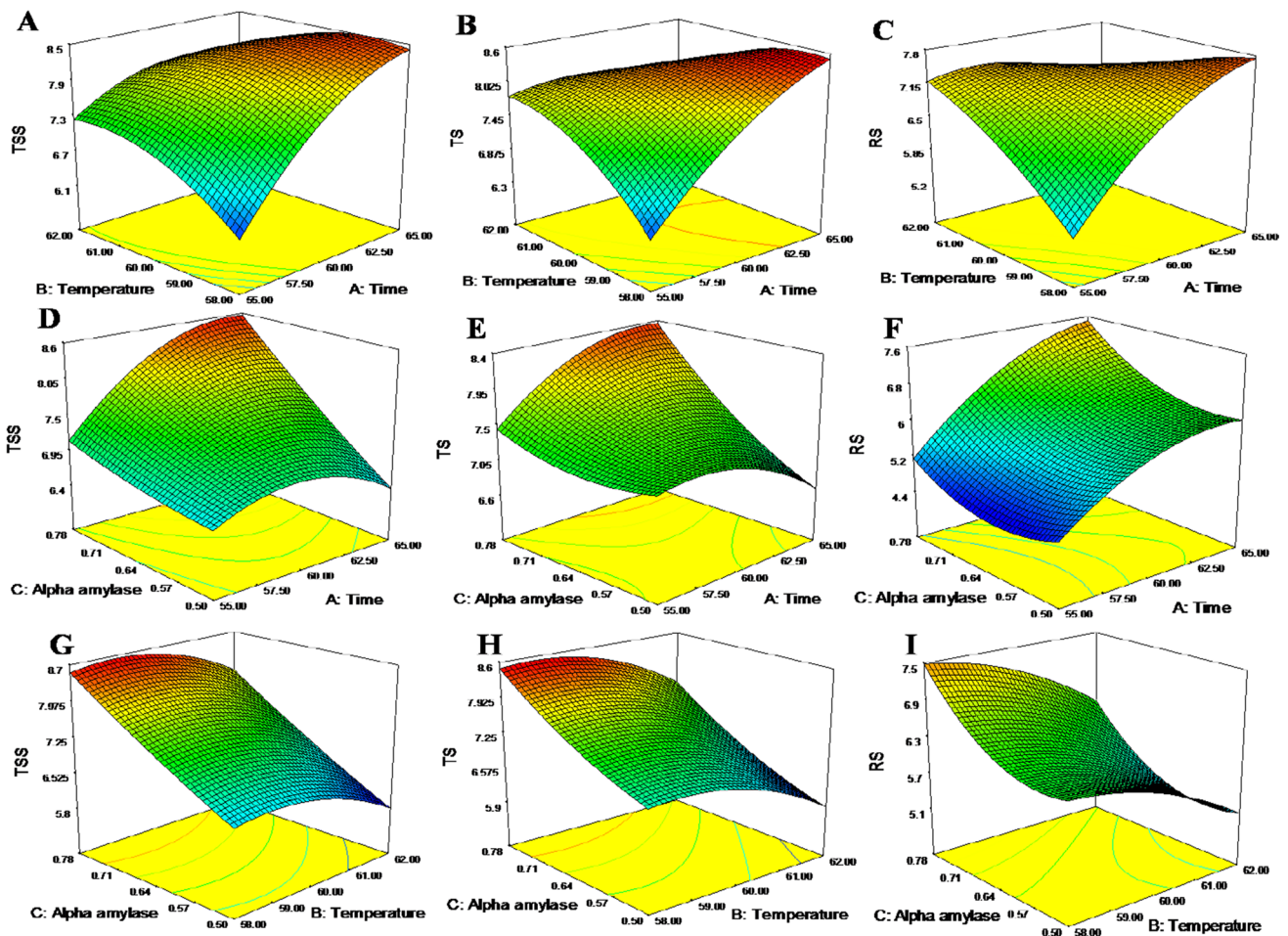
Fig. 2 Effect of process variables on total soluble solids (TSS) (**A**, **D**, **G**), total sugars (TS) (**B**, **E**, **H**), and reducing sugars (RS) (**C**, **F**, **I**) during liquefaction of potato waste

to specific temperature and time conditions. Reported optimum ranges for α-amylase activity encompass temperatures ranging from 55 to 60 °C, with corresponding time intervals falling within the range of 60 to 65 min [47].

The interactive impact of α-amylase dose and time on TSS, TS, and RS, while keeping the temperature at its median value, is shown in Fig. 2D, E, F. It was observed that simultaneous increases in α-amylase dose from 0.64 to 0.78% v/v and time from 58 to 63 min resulted in an increase in TSS, TS, and RS from 6.8 to 8.7 °Brix, 5.124 to 8.409 mg/mL, and 4.645 to 7.951 mg/mL. However, a further increase in α-amylase dose (> 0.78) and time (> 63) reduced the TSS (8.7–7.1 °Brix), TS (8.409–6.345 mg/mL), and RS (7.951–5.482 mg/mL). During liquefaction, high enzyme dosages and short processing durations hydrolyze starch quickly, putting the product at risk of deterioration and increased viscosity. Using too much enzyme and extending the liquefaction time might cause sugars to over-hydrolyze, making them less fermentable and increasing degradation risks and costs. However, utilizing too little enzyme

and short liquefaction durations may result in incomplete starch conversion, limiting efficiency and impeding enzyme activation. Finally, having inadequate enzyme with extended liquefaction times might slow down processes, requiring additional time and expense while correcting for restricted enzyme activity [48, 49].

The interactive effect of α-amylase dose and temperature on TSS, TS, and RS is depicted in Fig. 2G, H, I while maintaining the time at the centre point. Concentrations of TSS, TS, and RS increased from 7 to 8.7 °Brix, 6.452 to 8.409 mg/mL, and 5.932 to 7.951 mg/mL with a simultaneous rise in α-amylase dose (0.64–0.78% v/v) and temperature (56–60 °C). However, further increase in α-amylase dose (> 0.78% v/v) and temperature (> 65 °C) negatively affected TSS, TS, and RS, decreasing from 8.7 to 6.7 °Brix, 8.409 to 6.958 mg/mL, and 7.951 to 5.745 mg/mL. The lower TSS, TS, and RS concentrations (α-amylase dose > 0.78% v/v) can be attributed to reduced enzymatic efficiency and, consequently, lower glucose recovery. High enzyme doses and extreme temperatures during liquefaction can cause fast

starch hydrolysis, potentially surpassing acceptable conversion rates and resulting in glucose breakdown, product deterioration, and increased viscosity. When high enzyme doses are combined with low temperatures during liquefaction, enzymatic activity is marginally diminished. Although the compensating effect promotes effective starch breakdown, the process is slower than at higher temperatures. Low enzyme dosage and high temperature during liquefaction might result in inadequate starch hydrolysis, leaving unconverted starch and lowering fermentable sugar output. Prolonged exposure to high temperatures accelerates product breakdown [50].

3.4.2 Validation of developed RSM model

Validation experiments under the optimal condition were conducted to maximize the fermentable sugars release (Table 4). The predicted optimum conditions for maximum sugar release for liquefaction were 62.15 min, 59.8 °C, and 0.72% v/v (5000IU/mL/min) for time, temperature,

and α-amylase dose, respectively, corresponding to a TSS, TS, and RS concentration of 8.74 °Brix, 8.52 mg/mL, and 7.99 mg/mL, respectively. In a prior study, Aruwajoy et al. [51] identified optimal conditions for liquefaction as 95 °C temperature and 1 mL of α-amylase per 4.04 g dry weight of waste potato mash in 100 mL of deionized water.

3.5 Optimization of process parameters for saccharification by using RSM

3.5.1 Interactive effects of process parameters on TSS, TS, and RS during Saccharification

The findings in Table 4 illustrate a spectrum of values for TSS, TS, and RS in various experimental runs of saccharification processes (Fig. 3). TSS ranges were 8.1 to 14.8 °Brix; 8.767 to 13.501 mg/mL, TS; and 7.205 to 10.284 mg/mL, RS. Runs 1, 2, 3, 11, and 13 serve as representative median values for all inputs process. In contrast, run 15, executed with reduced time (17.2 h), temperature (50 °C),
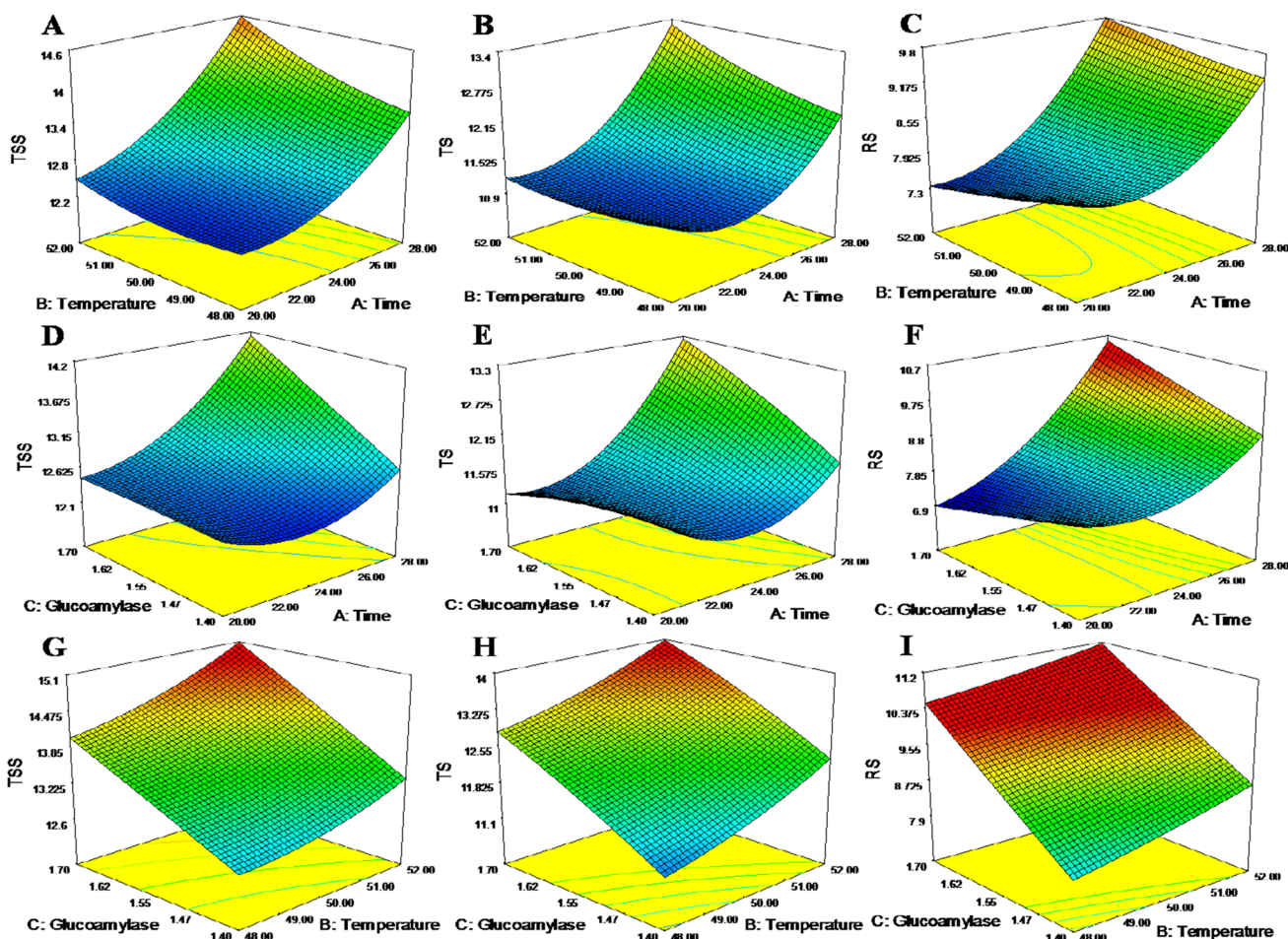

Fig. 3 Effect of process variables on total soluble solids (TSS) (**A**, **D**, **G**), total sugars (TS) (**B**, **E**, **H**), and reducing sugars (RS) (**C**, **F**, **I**) during saccharification of potato waste

and a glucoamylase (1000 IU/mL/min) dose of 1.78% v/v, yielded lower TSS (8.9 °Brix), TS (9.357 mg/mL), and RS (7.415 mg/mL). An extended time (28.5 h), higher temperature (50 °C), and increased glucoamylase dose of 1.6% (v/v) resulted in significantly enhanced yields of TSS, TS, and RS, reaching 14.8 °Brix, 13.501 mg/mL, and 10.284 mg/mL, respectively.

The graphs in Fig. 3A, B, C show how different process factors interact to affect TSS, TS, and RS during saccharification. An increase in time (24 to 28.5 h) and temperature (48 to 52 °C) resulted in an increase in TSS (10 to 14.7 °Brix), TS (10.892 to 13.51 mg/mL), and RS (8.421 to 10.284 mg/mL). Further increases in time (> 29 h) and temperature (> 52 °C) led to a decrease in TSS, TS, and RS to 9.7 °Brix, 9.216 mg/mL, and 7.822 mg/mL, respectively. The breakdown of glucoamylase (> 55 °C) in the current saccharification process affects TSS, TS, and RS due to temperature variations. Lower temperatures (< 52 °C for glucoamylase) reduce enzyme efficiency, negatively impacting sugar release. Optimal temperature and time conditions are crucial for maximizing glucoamylase reaction during both liquefaction and saccharification, with reported optimum ranges being 52 to 55 °C and 26.5 to 30 h, respectively [52]. Rani et al. [45] achieved a total reducing sugar content of 15.2% in potato flour hydrolysate through saccharification using glucoamylase (20.5 U/g starch) for 2 h at 60 °C. In an experiment conducted for optimizing temperature for bioethanol production from potato waste, it was observed that with increase in temperature from 25 to 37 °C, the ethanol amount also increased with maximum ethanol (34.5% v/v) obtained at 31 °C. Beyond 31 °C, a decrease in the yield of ethanol was observed due to the further conversion of other by-products [53] due to further conversion of other by-products.

The interactive impact of enzymatic dose and time on TSS, TS, and RS, while keeping the temperature at its median value, is shown in Fig. 3D, E, F. It was observed that simultaneous increases in glucoamylase dose from 1.60 to 1.72% (v/v) and time from 24 to 28.5 h showed an increase in TSS, TS, and RS from 10.5 to 14.7 °Brix, 11.152 to 13.501 mg/mL, and 8.456 to 10.284 mg/mL, respectively. Further increases in glucoamylase dose (> 1.72% v/v) and time (> 28.5) resulted in a decrease in TSS, TS, and RS from 14.7 to 10.1 °Brix, 13.501 to 10.467 mg/mL, and 10.284 to 7.952 mg/mL, respectively. Using too much enzyme and extended liquefaction times can over-hydrolyze sugars, making them less fermentable, increasing osmotic pressure, which raises the risks of degradation and costs. Using high enzyme dose and short liquefaction times may not fully convert starch, thus, reducing efficiency and hindering enzyme action. Lastly, having insufficient enzyme with long liquefaction times can slow down processes, requiring more time

and cost despite compensating for limited enzyme activity [48, 49].

In Fig. 3G, H, I, the combined impact of enzyme amount and temperature on TSS, TS, and RS is presented, keeping the time constant at the centre point. Increasing the enzymatic dose from 1.60 to 1.72% v/v and temperature from 50 to 55 °C led to an increase in TSS, TS, and RS from 10.2 to 14.7 °Brix, 10.845 to 13.501 mg/mL, and 8.266 to 10.284 mg/mL, respectively. However, further increments in glucoamylase dose (> 1.72% v/v) and temperature (> 55 °C) decreased the yield of TSS, TS, and RS from 14.7 to 9.8 °Brix, 13.501 to 9.725 mg/mL, and 10.284 to 7.821 mg/mL. The lower TSS, TS, and RS concentrations (glucoamylase dose > 1.72% v/v) can be attributed to reduced enzymatic efficiency and, consequently, lower glucose recovery. Research conducted by Dussan et al. [54] revealed that using a concentration of 1000 mg/L of glucoamylase at 67 °C not only significantly enhanced the yield of enzymatic hydrolysis of molasses but also demonstrated a twofold surge in the concentration of glucose liberated from molasses as the enzyme concentration escalated from 100 to 1000 mg/L. High enzyme dose and increased temperature can accelerate dextrin breakdown, achieving desired sugar levels quickly but posing risks of product degradation and increased viscosity. Although the compensatory effect allows efficient starch breakdown, the process is slower than at higher temperatures. Lower temperatures modestly slow the process compared to higher temperatures, but the high enzyme concentration remains effective in converting dextrins into fermentable sugars efficiently [50].

3.5.2 Validation of developed RSM model

Validation experiments under the optimal condition were conducted to maximize the TSS, TS, and RS. The optimal conditions for process were 28.5 h, 52 °C, and 1.7% (v/v) (1000 IU/mL/min) that lead to release of maximum TSS, TS, and RS to 14.8 °Brix, 13.75 mg/mL, and 10.72 mg/mL, respectively. In a prior study, Aruwajoye et al. [51] identified optimal conditions for saccharification as 60 °C temperature, 0.8 mL of amyloglucosidase, and 72 h duration time. Glucose conversion reached 34.9 g/L under these conditions. Sujeeta et al. [52] noted variations in glucose yield, attributing them to differences in agroresidual composition impacting enzymatic liquefaction and saccharification efficiency.

3.6 Fermentation and distillation

In the initial phase of fermentation at 28 °C, 92 mL of saccharified wort was inoculated with 6% *S. cerevisiae* MK680910, and exhibited total soluble solids (TSS), total sugars (TS), and reducing sugars (RS) as 14.7 °Brix, 13.75 mg/mL, and 10.72 mg/mL, respectively. Over the fermentation period

of 72 h, these sugar concentrations gradually decreased to 0 °Brix, 0.25 mg/mL, and 0.07 mg/mL, respectively, while there was a simultaneous increase in ethanol concentration to $7.7 \pm 0.10\%$. The pH was initially maintained at 5.6, but upon completion of the process, it decreased to 4.5. In a study by Dussan et al. [54], the highest ethanol yield (0.27%) was reported with a 1.0% potato processing waste (PPW) concentration, during a 72-h fermentation period at 35 °C with a 1.0% YPO3 inoculum. Additionally, Abouzied et al. [55] identified optimal ethanol production from potatoes when *Aspergillus niger* and *Saccharomyces cerevisiae* were co-cultured within a pH range of 5 to 6.

Following fermentation, the initial alcoholic wash, comprising 65.8 mL the resulting mixture, underwent primary fractional distillation at 80 °C. This process yielded a condensed fraction of 42.9 mL, with an ethanol content of 28.9% (v/v). Subsequently, a second fractional distillation of the primary distillate was conducted at the same temperature, resulting in the collection of an 18.7-mL condensed fraction with an increased ethanol content of 38.7% (v/v). Adhering to the specifications outlined by the Food Safety and Standards Authority of India (FSSAI), which mandates vodka to have an alcohol content falling within the range of 36 to 50% (v/v) or 65 to 87.5° proof, our product aligns precisely with these criteria at 38.7% (v/v) or 77.4° proof. This ethanol content falls within the approved ranges as per FSSAI guidelines, ensuring compliance with regulatory standards for the production of vodka.

Further, the vodka production from potato waste was validated at 2.5 L scale. Three hundred grammes of potato waste powder was obtained from 4.5 kg of potato waste. After mixing with water in a 1:7 ratio, it was subjected to enzymatic treatment under optimized conditions for release of fermentable sugars. The TSS value obtained in the upscaled wort was 14.7 °Brix. After allowing the wort to cool, it was inoculated with *S. cerevisiae* (MK680910) and fermented for 4 days at 28 °C in a 3-L fermentor. The alcohol content obtained after 4 days of fermentation was 7.6%. Following fermentation, the initial alcoholic wash, comprising 1.5 L, underwent primary fractional distillation at 80 °C. This process yielded a condensed fraction of 900 mL, with an ethanol content of 28.2% (v/v). Subsequently, a second fractional distillation of the primary distillate was conducted at the same temperature, resulting in the collection of 400 mL condensed fraction with an increased ethanol content of 38.4% (v/v). This culminated in the production of the final vodka, and possessing an acidity level of 0.24%.

4 Conclusion

This study reveals the potential of potato waste as a valuable source for vodka production. Proximate and physiochemical analysis showed the abundance of carbohydrates and other organic constituents in the waste. These were valorized for ethanol production. Liquefaction and saccharification were optimized by using RSM and after fermentation of saccharified waste under optimized conditions, an ethanol content of 7.6% (v/v) was obtained. After double distillation, an ethanol content of 38.4% (76.8 °P) was achieved. Thus, this study facilitates the adoption of a cost-effective fermentative processing of potato waste to vodka. This research invites further exploration into innovative ways of utilizing agricultural by-products, paving the way for a more environmentally conscious and resource-efficient future in the beverage industry.

Declarations

References

1. Wu T, Yan J, Liu R, Marcone MF, Aisa HA, Tsao R (2012) Optimization of microwave-assisted extraction of phenolics from potato and its downstream waste using orthogonal array design. Food Chem 133:1292–1298. https://doi.org/10.1016/j.foodchem.2011.08.002
2. Pathak PD, Mandavgane SA, Puranik NM, Jambhulkar SJ, Kulkarni BD (2018) Valorization of potato peel: a biorefinery approach. Crit Rev Biotechnol 38:218–230. https://doi.org/10.1080/07388551.2017.1331337
3. FAO (2021) Food and Agriculture Organization of the United Nations, FAOSTAT Statistical Database. https://www.fao.org/faostat/en/#data/QCL. Accessed 22 Nov 2023
4. Buckseth T, Tiwari JK, Singh RK, Kumar V, Sharma AK, Dalamu D, Bhardwaj V, Sood S, Kumar M, Sadawarti M, Challam C, Naik S, Pandey NK (2022) Advances in innovative seed potato production systems in India. Front Agron 4:1–7. https://doi.org/10.3389/fagro.2022.956667
5. Luthra V, Keshani, Kocher GS, Singh A (2024) Quality evaluation and Fourier transform infrared (FTIR) spectroscopy characterization of vodka produced from malted & un-malted potatoes using *Saccharomyces cerevisiae* (MK680910). Potato Research. https://doi.org/10.1007/s11540-024-09694-4
6. Abdelraof M, Hasanin MS, El-Saied H (2019) Ecofriendly green conversion of potato peel wastes to high productivity bacterial cellulose. Carbohydr Polym 211:75–83. https://doi.org/10.1016/j.carbpol.2019.01.095
7. Sharma S, Malhotra N, Singh A, Sharma R, Domínguez R, Lorenzo JM (2022) Modulation in techno-functional, textural properties, in vitro starch digestibility and macromolecular–structural

interactions of pasta with potato (*Solanum tuberosum* L). Molecules 27:7835. https://doi.org/10.3390/molecules27227835

8. Singh L, Kaur S, Aggarwal P (2023) Enhanced functional and textural properties of waffle premix by addition of phytonutrient-rich industrial potato waste. Biomass Conv Bioref 13: 14789–14802 (2023). https://doi.org/10.1007/s13399-022-03246-x

9. Singh L, Kaur S, Aggarwal P, Kaur N (2023b) Characterisation of industrial potato waste for suitability in food applications. Int J Food Sci Technol 58(5):2686–2694. https://doi.org/10.1111/ijfs.16023

10. Hamami Z, Javanbakht V (2023) Photocatalytic processes using potato peel extract-mediated CuO nanophotocatalyst for fast and efficient direct red 80 dye removal. Biomass Convers Biorefinery. https://doi.org/10.1007/s13399-023-05034-7

11. Kot AM, Pobiega K, Piwowarek K, Kieliszek M, Błażejak S, Gniewosz M, Lipińska E (2020) Biotechnological methods of management and utilization of potato industry waste- a review. Potato Res 63:431–447. https://doi.org/10.1007/s11540-019-09449-6

12. Yamada S, Shinomiya N, Ohba K, Sekikawa M, Oda Y (2009) Enzymatic hydrolysis and ethanol fermentation of by-products from potato processing plant. Food Sci Technol Res 15:653–658. https://doi.org/10.3136/fstr.15.653

13. Singh L, Kaur S, Aggarwal P (2022) Techno and bio functional characterization of industrial potato waste for formulation of phytonutrients rich snack product. Food Bioscience 49:101824. https://doi.org/10.1016/j.fbio.2022.101824

14. Felekis V, Stavraki C, Malamis D, Mai S, Barampouti EM (2023) Optimisation of bioethanol production in a potato processing industry. Fermentation 9:103. https://doi.org/10.3390/fermentation9020103

15. Israilides C, Vlyssides AG, Arapoglou D, Varzakas T, Marchant R, Vlysides AA (2008) Integrated management of potato starch wastes. In: Proceedings of the Waste and Resource Management – A Shared Responsibility (Waste 2008), September 16–17, Stratford-Upon-Avon, UK, No. 36

16. Sanchez OJ, Cardona CA (2008) Trends in biotechnological production of fuel ethanol from different feedstocks. Bioresource Technol 99:5270–5295. https://doi.org/10.1016/j.biortech.2007.11.013

17. Tasic MB, Konstantinovic BV, Lazic ML, Veljkovic VB (2009) The acid hydrolysis of potato tuber mash in bioethanol production. Biochem Eng J 43:208–211. https://doi.org/10.1016/j.bej.2008.09.019

18. Ruiz MI, Sanchez CI, Torrres RG, Molina DR (2011) Enzymatic hydrolysis of cassava starch for production of bioethanol with a Colombian wild yeast strain. Braz Chem Soc 22:2337–2343. https://doi.org/10.1590/S0103-50532011001200014

19. Shanavas S, Padmaja G, Moorthy SN, Sajeev MS, Sheriff JT (2011) Process optimization for bioethanol production from cassava starch using novel eco-friendly enzymes. Biomass Bioenergy 35(2):901–909. https://doi.org/10.1016/j.biombioe.2010.11.004

20. Fadel M (2000) Alcohol production from potato industry starchy waste. Egypt J Microbiol 35:273–287

21. Lamidi S, Olaleye N, Bankole Y, Obalola A, Aribike E, Adigun I (2022) Applications of response surface methodology (RSM) in product design, development, and process optimization *In* Response surface methodology- Research advances and application. Palanikumar Kayarogannam (Ed.), Intech Open. https://doi.org/10.5772/intechopen.106763

22. Montgomery DC (2005) Design and analysis of experiments: response surface method and designs. John Wiley and Sons, Inc, New Jersey

23. Breig SJM, Luti KJK (2021) Response surface methodology: a review on its applications and challenges in microbial cultures. Mater Today: Proc 42: 2277–2284. https://doi.org/10.1016/j.matpr.2020.12.316

24. Yolmeh M, Jafari SM (2017) Applications of response surface methodology in the food industry processes. Food Bioprocess Technol 10(3):413–433

25. Bobade H, Singh A, Sharma S, Gupta A, Singh B (2022) Effect of extrusion conditions and honey on functionality and bioactive composition of whole wheat flour-based expanded snacks. J Food Process Preserv 46:e16132. https://doi.org/10.1111/jfpp.16132

26. Bansal R, Katyal P, Jain D (2022) Enzymatic and acidic hydrolysis of cull potatoes for production of fermentable sugars. Starch - Stärke 74:2100202. https://doi.org/10.1002/star.202100202

27. AACC (2000) Approved methods of American Association of Cereal Chemists. 10th Edn.The Association St. Paul, MN. https://doi.org/10.4236/sm.2023.134014

28. Clegg K (1956) The application of anthrone reagent to the estimation of starch in cereals. J Sci Food Agric 7:40–44. https://doi.org/10.1002/jsfa.2740070108

29. Dubois M, Gilles KA, Hamilton JK, Rebers PA, Smith F (1956) Colorimetric method for determination of sugars and related substances. Anal Chem 28:350–356. https://doi.org/10.1021/ac60111a017

30. Miller GL (1959) Use of dinitrosalicylic acid reagent for determination of reducing sugars. AnalChem 31:426–28. https://doi.org/10.1021/ac60147a030

31. Singh P, Kaur G, Singh A, Sharma T, Dar BN (2023) Improved mechanical, functional and antimicrobial properties of corn starch-based biodegradable nanocomposites films reinforced with lemongrass oil nanoemulsion and starch nano-crystal. Mater Chem Phys 308:128267. https://doi.org/10.1016/j.matchemphys.2023.128267

32. Sharma T, Kaur G, Singh A, Singh P (2023) Montmorillonite and chitosan modulates the techno-functional, mechanical, antibacterial, biodegradation and morphological characteristics of gluten-based nanocomposite films. J Food Meas Charact 17(6):5550–5568. https://doi.org/10.1007/s11694-023-02062-9

33. Azizi AF, Sethi S, Joshi A, Singh AM, Raigond P, Singh MK, Yadav RK (2020) Biochemical and functional attributes of raw and boiled potato flesh and peel powders for suitability in food applications. JFST 57:3955–3965. https://doi.org/10.1007/s13197-020-04424-3

34. Liang S, Han Y, Wei L et al (2015) Production and characterization of bio-oil and bio-char from pyrolysis of potato peel wastes. Biomass Convers Bior 5:237–246. https://doi.org/10.1007/s13399-014-0130-x

35. Akyol H, Riciputi Y, Capanoglu E, Caboni MF, Verardo V (2016) Phenolic compounds in the potato and its byproducts: an overview. Int J Mol Sci 17:835. https://doi.org/10.3390/ijms17060835

36. Javed A, Ahmad A, Tahir A, Shabbir U, Nouman M, Hameed A (2019) Potato peel waste its nutraceutical, industrial and biotechnological applications. AIMS Agric Food 4:3807–3823. https://doi.org/10.3934/agrfood.2019.3.807

37. Adeboye PT, Bettiga M, Olsson L (2014) The chemical nature of phenolic compounds determines their toxicity and induces distinct physiological responses *in Saccharomyces cerevisiae* in lignocellulose hydrolysates. AMB Express 4:46. https://doi.org/10.1186/s13568-014-0046-7

38. Raina S, Gupta A, Singh A, Surasani VKR, Sharma S (2023) Functionality of pasta enriched with pumpkin seed meal: cooking quality, techno-functional properties, textural and structural characterisation. Int J Food Sci Technol 58(5):2735–2743. https://doi.org/10.1111/ijfs.16077

39. Saini M, Singh A, Sharma T, Surasani VKR, Kumar V, Bobade H (2024) Enrichment of pasta with *Pangasianodon hypophthalmus* protein isolate for improved sustainability, nutrition, and quality. Int J Food Sci Technol 59(2):1160–1168. https://doi.org/10.1111/ijfs.16756

40. Singh G, Singh B, Singh A, Kumar V, Surasani VKR (2024) Development and characterisation of barley-based non-conventional pasta supplemented with chickpea flour. Int J Food Sci Technol 59(2):1104–1112. https://doi.org/10.1111/ijfs.16553

41. Kaur A, Singh A, Kaur H, Gupta A, Surasani VKR, Dhaliwal SS (2024) Influence of different processing conditions on nutritional, phytochemical, and physical properties of aquatic fern (*Azolla pinnata*): a sustainable nutrient-rich human food. FS&T 4(2):344–354. https://doi.org/10.1021/acsfoodscitech.3c00458

42. Dudeja I, Mankoo RK, Singh A, Kaur J (2023) Development, characterisation and biodegradability of rice straw lignin based sustainable biopolymeric films. IJFST 58(5):2754–2763. https://doi.org/10.1111/ijfs.16105

43. Kapil S, Mankoo RK, Dudeja I, Singh A, Kaur J (2023) Structural, antioxidant, antibacterial and biodegradation properties of rice straw xylan (native and modified) based biofilms. IJFST 58(5):2772–2781. https://doi.org/10.1111/ijfs.16118

44. Chouhan NA, Aruwajoye GS, Sewsynker-Sukai Y, Kana EG (2020) Valorisation of potato peel wastes for bioethanol production using simultaneous saccharification and fermentation: process optimization and kinetic assessment. Renewable Energy 146:1031–1040. https://doi.org/10.1016/j.renene.2019.07.042

45. Rani P, Sharma S, Garg FC, Raj K, Wati L (2010) Ethanol production from potato flour by *Saccharomyces cerevisiae*. Indian J Sci Technol 3:733–736. https://doi.org/10.17485/ijst/2010/v3i7/29804

46. Betiku E, Akindolani O, Ismaila AR (2013) Enzymatic hydrolysis optimization of sweet potato (Ipomoea batatas) peel using a statistical approach. Brazilian J Chem Engg 30:467–476

47. Izmirlioglu G, Demirci A (2012) Ethanol production from waste potato mash by using *Saccharomyces*. Appl Sci 144:738–753. https://doi.org/10.3390/app2040738

48. Permanasari AR, Yulistiani F, Purnama RW, Widjaja T, Gunawan S (2018) The effect of substrate and enzyme concentration on the glucose syrup production from red sorghum starch by enzymatic hydrolysis. IOP Conf Series: Earth Environ Sci 160: 012002. https://doi.org/10.1088/1755-1315/160/1/012002

49. Arif AB, Sasmitaloka KS, Winarti C (2019) Effect of liquefaction time and enzyme addition on liquid sugar production from sweet sorghum starch by enzymatic hydrolysis. IOP Conf Series: Earth Environ Sci 250: 012042. https://doi.org/10.1088/1755-1315/250/1/012042

50. Pele GI, Bolade MK, Enujiugha VN, Sanni DM, Ogunsua AO (2018) Effect of pH and temperature on the activities of α-amylase in cassava starch liquefaction. AJFST 9(2):37–42. https://doi.org/10.14303/ajfst.2018.233

51. Aruwajoye GS, Sewsynker-Sukai Y, Kana EG (2020) Valorisation of cassava peels through simultaneous saccharification and ethanol production: effect of prehydrolysis time, kinetic assessment and preliminary scale up. Fuel 278:11835. https://doi.org/10.1016/j.fuel.2020.118351

52. Sujeeta, Kamla M, Mehta S, Sihag K (2017) Isolation and screening of amylase producing fungi. Int J Curr Microbiol App Sci 6:783–788. https://doi.org/10.20546/ijcmas.2017.604.098

53. Tenkolu GA, Kuf KD, Gindaba GT (2022) Optimization of fermentation condition in bioethanol production from waste potato and product characterization. BMC 1–19. https://doi.org/10.1007/s13399-022-02974-4

54. Dussan KJ, Silva DD, Moraes EJ, Arruda PV, Felipe MG (2014) Dilute-acid hydrolysis of cellulose to glucose from sugarcane bagasse. Chem Eng Trans 38:433–438. https://doi.org/10.3303/CET1438073

55. Abouzied MM, Reddy CA (1987) Fermentation of starch to ethanol by a complementary mixture of an amylolytic yeast and *Saccharomyces cerevisiae*. Biotechnol Lett 9:59–62. https://doi.org/10.1007/BF01043395